STRUCTURAL CONTROL AND HEALTH MONITORING
Struct. Control Health Monit. 2009; **16**:509–529
Published online 9 February 2009 in Wiley InterScience (www.interscience.wiley.com). DOI: 10.1002/stc.301

Benchmark structural control problem for a seismically excited highway bridge—Part I: Phase I Problem definition

Anil Agrawal[1,*,†,‡], Ping Tan[2,‡], Satish Nagarajaiah[3,4,‡] and Jian Zhang[5,§]

[1]*Department of Civil Engineering, The City College of the City University of New York, T-121 Steinman Hall, Convent Avenue at 140th Street, New York, NY 10031, U.S.A.*
[2]*Earthquake Engineering Research and Test Center, Guangzhou University, Guangzhou, Guangdong, China*
[3]*Department of Civil and Environmental Engineering, Rice University, Houston, TX 77005, U.S.A.*
[4]*Department of Mechanical Engineering and Materials Science, Rice University, Houston, TX 77005, U.S.A.*
[5]*Department of Civil and Environmental Engineering, University of California, Los Angeles, CA 90095, U.S.A.*

SUMMARY

This paper presents the problem definition of the benchmark structural control problem for the seismically excited highway bridge. The benchmark problem is based on the newly constructed 91/5 highway over-crossing in southern California. The goal of this benchmark effort is to develop a standardized model of a highway bridge using which competing control strategies, including devices, algorithms and sensors, can be evaluated comparatively. To achieve this goal, a 3D finite-element model is developed in MATLAB to represent the complex behavior of the full-scale highway over-crossing. The nonlinear behavior of center columns and isolation bearings is considered in formulating the bilinear force–deformation relationship. The effect of soil–structure interaction is considered by modeling the interaction by equivalent spring and dashpot. The ground motions are considered to be applied simultaneously in two directions. A MATLAB-based nonlinear structural analysis tool has been developed and made available for nonlinear dynamic analysis. Control devices are assumed to be installed between the deck and the end abutments of the bridge. Evaluation criteria and control constraints are specified for the design of controllers. Passive, semi-active and active devices and algorithms can be used to study the benchmark model. The participants in this benchmark study are required to define their control devices, sensors and control algorithms, evaluate and report the results of their proposed control strategies. Copyright © 2009 John Wiley & Sons, Ltd.

KEY WORDS: structural response control; seismically excited highway bridge; highway bridge benchmark problem; earthquake response control; smart protective systems

*Correspondence to: Anil Agrawal, Department of Civil Engineering, The City College of the City University of New York, T-121 Steinman Hall, Convent Avenue at 140th Street, New York, NY 10031, U.S.A.
†E-mail: agrawal@ccny.cuny.edu, anil@ce.ccny.cuny.edu
‡Professor.
§Assistant Professor.

Contract/grant sponsor: National Science Foundation; contract/grant number: CMS 0099895
Contract/grant sponsor: ASCE Committee on Structural Control
Contract/grant sponsor: International Association of Structural Control and Monitoring

Received 29 March 2008
Revised 14 October 2008
Accepted 15 October 2008

1. INTRODUCTION

A variety of passive, active, semi-active and hybrid control strategies have been proposed as a means for alleviating seismic or wind responses of buildings and bridges during last several decades. In order to make a systematic and objective comparison of various control strategies, benchmark problems, which are well-defined analytical 'test beds' implemented in MATLAB environment, have been developed to allow researchers to apply their control strategies and measure the response quantities to a set of standardized loads in terms of prescribed performance criteria [1].

There have been several structural control benchmark problems defined so far for investigating the effectiveness of various control strategies for a series of civil engineering structures, most of which are focused on the control of building structures. The first generation of seismically excited benchmark building models was developed in 1998 by Spencer *et al.* [2]. Following this study, seismically-excited and wind-excited benchmark building models have been developed by Spencer *et al.* [3], Ohtori *et al.* [4] and Yang *et al.* [5]. Contributions to seismically-excited and wind-excited building models have been published in the Volume 130, No. 4 of the *Journal of Engineering Mechanics* (ASCE) in 2004. Dyke *et al.* [6] and Caicedo *et al.* [7] have developed benchmark cable-stayed bridge problem. Papers that contributed to the benchmark cable-stayed bridge study have been published in Volume 10 of *Journal of Structural Control* in 2003. More recently, two phases of the benchmark model for base-isolated building have been developed by Narasimhan *et al.* [8], Nagarajaiah and Narasimhan [9] and Narasimhan *et al.* [10,11]. Contributions to this benchmark study have been published in Volume 13, No. 2–3, Year 2006 and Volume 15, No. 5, Year 2008 of the *Structural Control and Health Monitoring Journal*.

A highway over-crossing or bridge, connecting major transportation routes, is a key node in transportation network. It must continue to function after an earthquake. Therefore, a higher level of performance with less structural damage is required for such bridges. Recent earthquakes such as Northridge and Kobe have demonstrated the importance of maintaining the operation of bridge structures. To deal with seismic risk to bridges, seismic upgrading of critical highways is under way by various state and federal agencies, and considerable attention has been paid to research and development of effective protective systems. For highway bridges, seismic isolation bearings in combination with passive, semi-active and active control systems are used as protective systems [12–14]. Seismic isolation bearings, which usually replace conventional bridge bearings, decouple the superstructure from piers and abutments during earthquakes, thereby significantly reducing the seismic forces induced in the bridge structure and lowering the strength and ductility demands on the bridge [12,14–17]. However, nonlinear behavior of the bridge columns or excessive displacement of bearings during near-fault ground motions may result in significant damage to the bridge with isolation bearings. It has been demonstrated by several researchers that passive, semi-active and active control systems installed in parallel with isolation bearings are capable of reducing excessive displacement of bearings or significant damage to bridge piers due to nonlinear behavior [14,18,19]. Hence, it is important to investigate the comparative effectiveness of various protective systems in reducing response quantities of highway bridges.

To meet this objective, it was decided to develop a benchmark structural control model for highway bridges during the meeting of the ASCE Committee on Structural Control during the 2003 Structures Congress in Seattle. This paper presents the problem definition for the

DOI: 10.1002/stc

benchmark highway bridge. The highway bridge model is based on the newly constructed 91/5 highway bridge in southern California and has been developed to provide a systematic and a standardized means by which competing control strategies, including devices, control algorithms and sensors, can be evaluated. The benchmark package consists of the MATLAB-based 3D finite-element model of the highway bridge, design of sample controllers, prescribed ground motions and a set of evaluation criteria.

In previous benchmark models of buildings and cable-stayed bridge, an evaluation model was developed by condensing the full-order system. All numerical simulations, including implementation of control strategies, were conducted on the condensed evaluation model. In the present benchmark model of highway bridge, full-order nonlinear model of the bridge has been used as the evaluation model of the bridge to preserve the effects of column nonlinearity and a realistic implementation of the control system.

In the modeling of the bridge, the behavior of center bent columns and isolators is assumed to be bilinear (inelastic). The effects of soil–structure interaction at the end abutments/approach embankments are considered. The ground motions are considered to be applied to the bridge simultaneously in two directions. To facilitate direct comparison of the relative merits of various control strategies, a set of 21 evaluation criteria are defined to measure the effectiveness of the control strategies, along with the associated control design constraints. The participants of this benchmark study are encouraged to propose new control strategies or applications of proven effective strategies. These strategies may be passive, active, semi-active or their combination. Researchers participating in this benchmark problem will be required to define their control devices, sensors and algorithms and evaluate the effectiveness of their proposed control strategies critically. The problem statement and MATLAB program are available on the benchmark web site http://www-ce.engr.ccny.cuny.edu/People/Agrawal.

2. BENCHMARK HIGHWAY BRIDGE

The highway bridge used for this benchmark study is the newly constructed 91/5 over-crossing, located in Orange County of Southern California. Figure 1 shows the photograph of the bridge. It is

Figure 1. View of 91/5 highway over-crossing.

DOI: 10.1002/stc

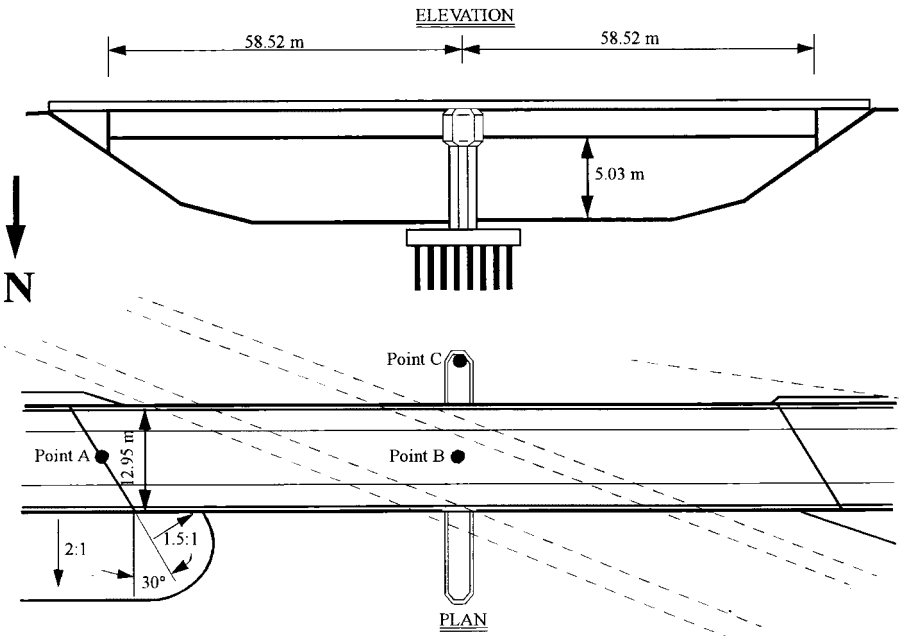

Figure 2. Elevation and plan views of 91/5 over-crossing.

a continuous two-span, cast-in-place prestressed concrete box-girder bridge. The elevation and plan views of the bridge are illustrated in Figure 2. The Whittier–Ellsinore fault is 11.6 km (7.2 miles) to the northeast, and the Newport–Inglewood fault zone is 20 km (12.5 miles) to the southwest of the bridge.

The bridge has two spans, each of 58.5 m (192 ft) long, spanning a four-lane highway and has two abutments skewed at 33°. The width of the deck along east span is 12.95 m (42.5 ft) and it is 15 m (49.2 ft) along west direction. The cross section of the deck consists of three cells. The deck is supported by a 31.4 m (103 ft) long and 6.9 m (22.5 ft) high prestressed outrigger, which rests on two pile groups, each consisting of 49 driven concrete friction piles. The columns are approximately 6.9 m (22.5 ft) high. The cross section of the bridge along the outrigger and a plan view of the pile group are shown in Figure 3.

The pile groups at both end abutments consist of vertical and battered piles. Figure 4 shows the pile group configuration at the east end abutments. The bridge deck is isolated using four traditional non-seismic elastomeric pads at each abutment, and the total eight fluid dampers are installed between the end abutments and deck (four dampers at each end) to reduce seismic responses. Figure 5 shows the idealized model of the bridge, its approach embankments and pile foundations. Note that the approach embankment is modeled by constant spring and dashpots.

3. EVALUATION MODEL

3.1. Description of finite-element model

In the evaluation model, lead rubber bearings are used to replace eight traditional non-seismic elastomeric pads, since the seismic isolation bearing (lead rubber bearings) can provide

DOI: 10.1002/stc

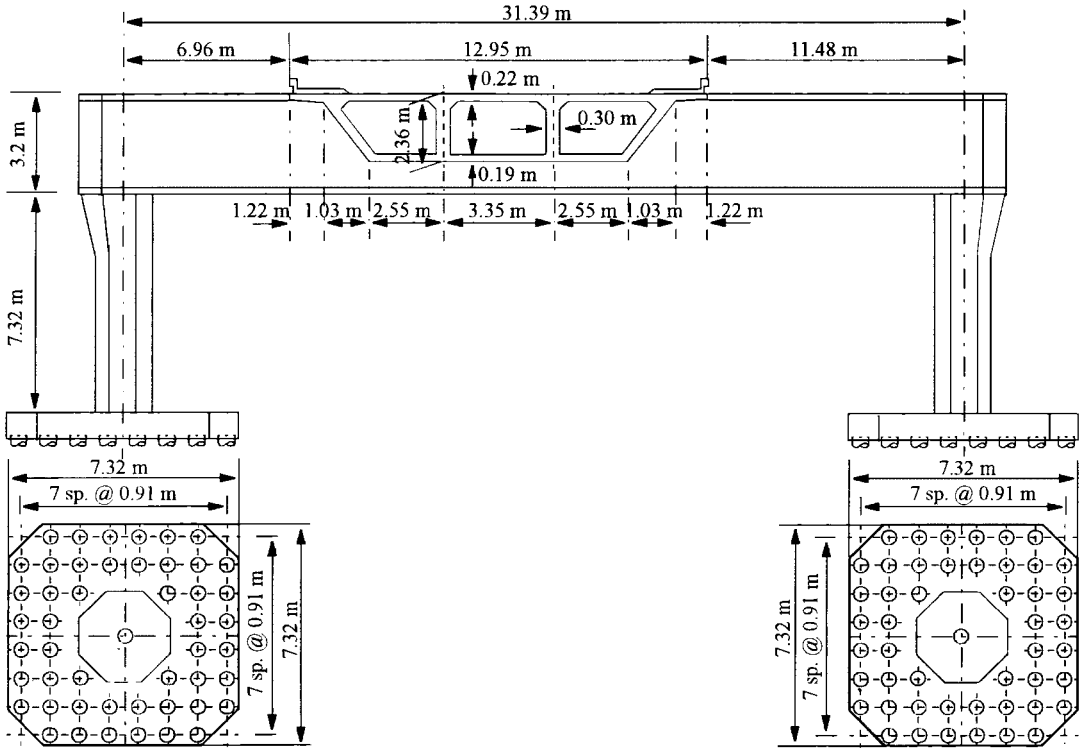

Figure 3. Cross section of 91/5 over-crossing and configuration of pile groups at center bent.

improved seismic performance. Consequently, passive fluid dampers (originally installed in the bridge on 91/5 over-crossing) are not considered to be installed in the evaluation model. Control devices are to be installed between the deck and the end abutments of the bridge to investigate their effectiveness. A 3D finite-element model, shown in Figure 6, has been developed in ABAQUS [20], which is representative of the actual bridge. The finite-element model has a total of 108 nodes, 4 rigid links, 70 beam elements, 24 springs, 27 dashpots and 8 user-defined bearing elements. The superstructure of the bridge, including the deck and the bent beam, is assumed to be elastic. Both the abutments and deck-ends are assumed to be rigid and have a skew angle of 33°. Structural member nonlinearities are included to capture the inelastic moment–curvature behavior of columns and shear–displacement relationship of bearings.

The bridge superstructure is represented by 3D beam elements. In ABAQUS, the B31 beam element was chosen to model the deck and the bent. Rigid links are used to model the abutments and deck-ends. The effects of soil–structure interaction at the end abutments/approach embankments are included by frequency-independent springs and dashpots [21].

The beam elements are located at the center of gravity of members, whose cross-section properties are obtained from geometric data without considering any cracked section reduction. The total mass of the superstructure includes all the non-structural elements, although their stiffness contribution is neglected. At both ends of the bridge, rigid links with a skew angle of 33° are used to connect the isolation bearings and control devices between the deck and the abutment.

DOI: 10.1002/stc

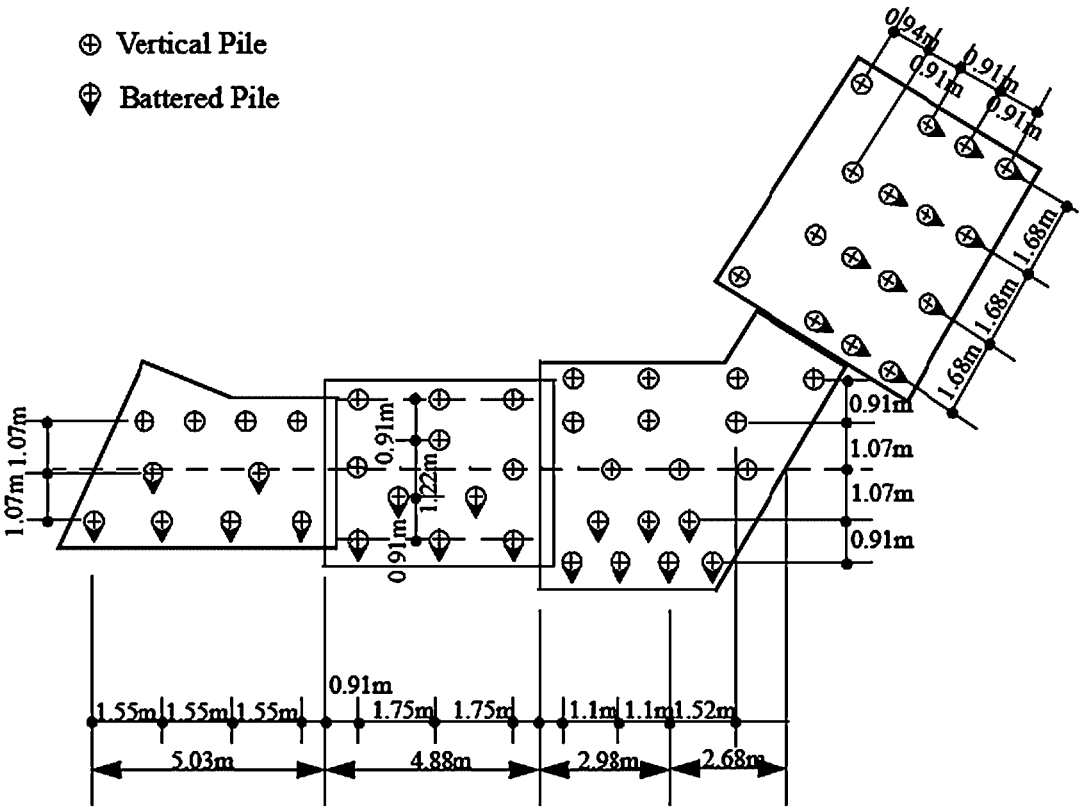

Figure 4. Plan view of pile groups at east abutments.

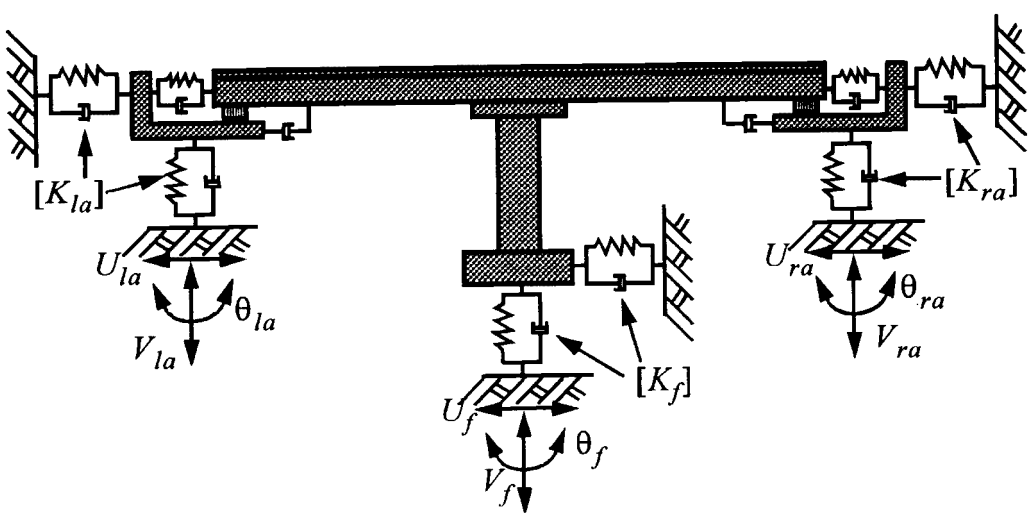

Figure 5. Elevation view of idealized model.

DOI: 10.1002/stc

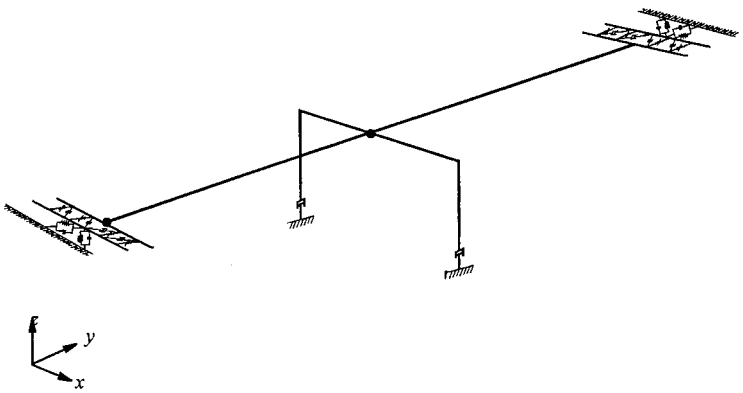

Figure 6. The 3D finite-element model of bridge.

Each column of the bent is modeled as stiff column cap, elastic column segments and nonlinear column segments, which are all modeled by B31 element since this element can model the nonlinearity of the member. The pile group under bent columns is also modeled by a B31 beam element. This beam element has appropriate cross section to give correct static translational and rotational stiffnesses. Three dashpots are used to simulate the soil radiation damping in the three translational directions.

There are totally eight bearings between bridge deck and abutments to isolate the bridge superstructure at both abutment-ends. The bearings are idealized by bi-directional bilinear plasticity model as described by Makris and Zhang [21]. This model is written as a user-defined subroutine within ABAQUS. The bearings are modeled as shear element, i.e. the vertical axial stiffness of the bearings is taken as infinite, and their torsional rigidity and bending stiffness are assumed to be zero. The shear force–displacement relationship in two horizontal directions is considered to be bilinear. The mass and damping of the isolation bearings are neglected.

Approach embankments on each side of the bridge are massive, long deformable bodies that have a tendency to amplify considerably the free-field earthquake motions and interact strongly with the bridge structure. Accordingly, the assessment of the efficiency of the seismic protection devices by accounting for the effects of soil–structure interaction at the end abutments/approach embankments is necessary. A sufficiently accurate consideration of the approach embankments can be obtained if the soil stiffness and damping coefficients are evaluated by frequency-independent spring and dashpot constants. The pile foundations at both abutments are assumed to behave as an equivalent linear visco-elastic element, and are modeled as springs and dashpots in both horizontal directions. Thus, the combined spring and dashpot values are obtained to account for the presence of embankment and pile foundation at both ends of the bridge.

After the 3D FEM model was developed in ABAQUS, a natural frequency analysis was performed. The first six natural frequencies of vibration of the finite element model (FEM) model are displayed in Table I, and the representative mode shape for the first six modes is shown in Figure 7. It is observed that the first mode is torsional with a natural frequency of 1.23 Hz. The second mode is a torsional mode coupled with vertical. The third and the fourth modes are first vertical and transverse and the fifth and sixth modes are second vertical and transverse, respectively.

DOI: 10.1002/stc

Table I. Natural frequencies of the FEM model.

Mode no.	Frequency (Hz)	Mode
1	1.23	Torsional
2	1.28	Torsional+vertical
3	1.55	Vertical
4	1.69	Transverse
5	1.77	Second vertical
6	3.26	Second transverse

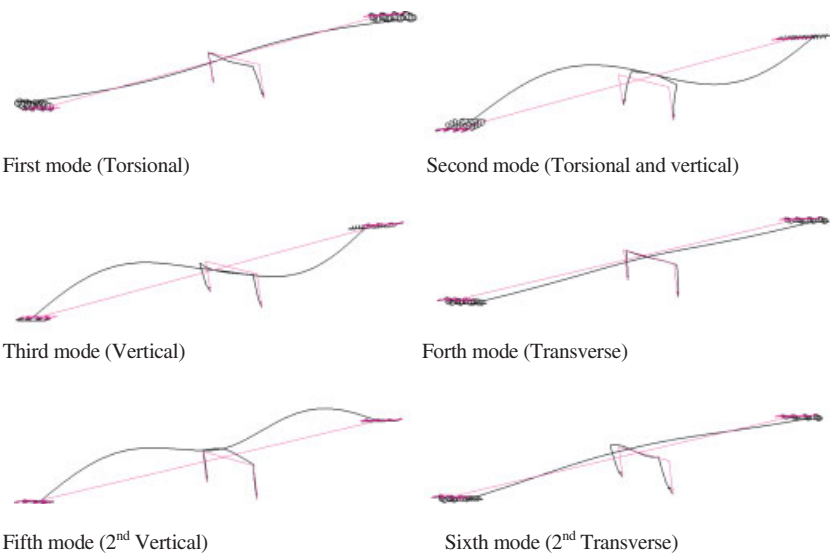

Figure 7. Six mode shapes of the 3D bridge model.

3.2. MATLAB implementation

All element mass matrices and initial elastic element stiffness matrices obtained in ABAQUS are summed at nodal masses to assemble global stiffness and mass matrices within MATLAB environment [22], and then the nonlinear elements are modeled for generating the evaluation model. Each nodal mass of the deck and the bent was assigned six dynamic degrees of freedom (DOF). The deck-ends and abutments, which are assumed to be infinitely rigid in plane, are modeled using three master DOF (two translational and one torsional DOF). The full nonlinear model of the bridge has 430 DOF. This model is used as the evaluation model of the bridge.

The global damping matrix C can be expressed as a combination of the distributed 'inherent' damping in the structure and soil radiation damping. The inherent damping of the superstructure is assumed to be a function of the mass and initial elastic stiffness matrix of the superstructure. The Raleigh damping parameters are computed by assuming a 5% modal damping ratio in the first and second modes.

DOI: 10.1002/stc

The nonlinear moment–curvature behavior of the two center columns is modeled by a bilinear hysteresis model. For simplification, the force–deformation relations for axial, shear and torsional behavior are assumed to be linear and only bending moment–curvature relationships in two directions are considered to be bilinear. The interaction between the axial load and bending moment during earthquake motions is not included. Besides, the nonlinear responses in both directions are considered to be uncoupled. This assumption is reasonable since the responses of columns are dominated by bending.

A concentrated plasticity model has been implemented for modeling the material nonlinearity of the bent column [23]. The plastic deformations over an element are assumed to be concentrated at the ends of the member. The moment–curvature relationship in both directions is idealized as bilinear and composed of two components: linear and elasto-plastic component. The elastic behavior remains unchanged, while the moments and shears of the elasto-plastic member are the combination of the end forces of the components according to the state of yield. As the plastic formulation in one direction has four possibilities: a hinge at the i-end, at the j-end, at both the ends or no hinge, there are totally 16 possibilities of states of yield for a beam segment. Thus, the incremental moments and shears at both ends of the nonlinear column element can be expressed as

$$\begin{bmatrix} \Delta V_{y,i} \\ \Delta V_{z,i} \\ \Delta M_{z,i} \\ \Delta M_{y,i} \\ \Delta V_{y,j} \\ \Delta V_{z,j} \\ \Delta M_{z,j} \\ \Delta M_{y,j} \end{bmatrix} = (pK_{\mathrm{e}} + qK_{\mathrm{p}}^{m}) \begin{bmatrix} \Delta v_{y,i} \\ \Delta v_{z,i} \\ \Delta \theta_{z,i} \\ \Delta \theta_{y,i} \\ \Delta v_{y,j} \\ \Delta v_{z,j} \\ \Delta \theta_{z,j} \\ \Delta \theta_{y,j} \end{bmatrix} \tag{1}$$

where K_{e} is the element elastic stiffness matrix, K_{p}^{m} is the element plastic stiffness matrix and m is the state of yield, i.e. $m = 1$, or 2,…, or 16. In Equation (1), p and q are the fractions of bending stiffness apportioned to the linear and elasto-plastic components, respectively, and $p+q = 1$. The total element stiffness is equal to the sum of K_{e} and K_{p}^{m}. The stiffness K_{e} is the constant linear component of the nonlinear member stiffness, while the plastic stiffness K_{p}^{m} is determined as the member ends are assumed to behave as a real center hinge. Consequently, K_{p}^{m} is quite different for each possible yield state. Hence, total element stiffness matrix changes at each increment of time during the nonlinear dynamic analysis.

The bilinear shear force–deformation relationship of the bearing in two horizontal directions is defined below as follows:

$$\begin{aligned} F_x &= K_{\mathrm{p}x} U_x + (K_{\mathrm{e}x} - K_{\mathrm{p}x})\bar{U}_x \\ F_y &= K_{\mathrm{p}y} U_y + (K_{\mathrm{e}y} - K_{\mathrm{p}y})\bar{U}_y \end{aligned} \tag{2}$$

In Equation (2), F_x is the restoring force of isolation bearings in the x direction, F_y is the restoring force of isolation bearings in the y direction, $K_{\mathrm{p}x}$ is the post-yield stiffness of isolation bearings in the x direction, $K_{\mathrm{p}y}$ is the post-yield stiffness of isolation bearings in the y direction,

DOI: 10.1002/stc

K_{ex} is the pre-yield stiffness of isolation bearings in the x direction, K_{ey} is the pre-yield stiffness of isolation bearings in the y direction, $\bar{U}_x$ is the yield displacement of the bearing in the x direction and $\bar{U}_y$ is the yield displacement of the bearing in the y direction. The bilinear force–deformation relationship in Equation (2) is hysteretic in both directions. However, the bilinear hystereses in x and y directions are not coupled, i.e. restoring force in the x direction only depends on the deformation in the x direction.

4. THE 3D NONLINEAR DYNAMIC ANALYSIS

The incremental equation of dynamic equilibrium for the nonlinear evaluation model can be expressed in the following form:

$$M\Delta\ddot{U}(t) + C\Delta\dot{U}(t) + K(t)\Delta U(t) = -M\eta\Delta\ddot{U}_g(t) + b\Delta F(t) \tag{3}$$

where ΔU is the incremental displacement vector, $\ddot{U}_g$ is the vector of ground accelerations, including two horizontal components, and $\Delta F(t)$ is the incremental control force. In Equation (3), η and b are loading vectors for the ground acceleration and control forces, respectively, and M is the mass matrix. The stiffness matrix of the structure, $K(t)$, consists of the linear part K_L and the nonlinear part $K_N(t)$. Equation (3) can be solved using the general Newmark integration method [24], which may be expressed as

$$\dot{U}(t+\Delta t) = \dot{U}(t) + [(1-\delta)\ddot{U}(t) + \delta\ddot{U}(t+\Delta t)]\Delta t \tag{4}$$

$$U(t+\Delta t) = U(t) + \dot{U}(t)\Delta t + [(\tfrac{1}{2}-\alpha)\ddot{U}(t) + \alpha\ddot{U}(t+\Delta t)](\Delta t)^2 \tag{5}$$

where α and δ are parameters that can be determined to obtain integration accuracy and stability. When $\delta = \frac{1}{2}$ and $\alpha = \frac{1}{4}$, the calculations are unconditionally stable and they do not introduce any numerical damping [25]. The Newmark integration method becomes the constant-average acceleration method for δ and α selected above. The incremental displacement ΔU can be solved from the following equation:

$$\Delta\bar{K}\Delta U = \Delta\bar{P} \tag{6}$$

in which $\Delta\bar{K}$ and $\Delta\bar{P}$ are the equivalent dynamic stiffness and load vector given by

$$\Delta\bar{K} = \frac{1}{\alpha(\Delta t)^2}M + \frac{\delta}{\alpha\Delta t}C + K(t) \tag{7}$$

$$\Delta\bar{P} = -M\eta\Delta\ddot{U}_g(t) + b\Delta F(t) + M\left[\frac{1}{\alpha\Delta t}\dot{U}(t) + \frac{1}{2\alpha}\ddot{U}(t)\right] + C\left[\frac{\delta}{\alpha}\dot{U}(t) + \frac{\Delta t}{2}\left(\frac{\delta}{\alpha}-2\right)\ddot{U}(t)\right] \tag{8}$$

The incremental velocity can be obtained from the following equation:

$$\Delta\dot{U} = \frac{\delta}{\alpha\Delta t}\Delta U - \frac{\delta}{\alpha}\dot{U}(t) + \left(1-\frac{\delta}{2\alpha}\right)\Delta t\ddot{U}(t) \tag{9}$$

In order to reduce the accumulated error, the increment of acceleration is solved directly from the dynamic equation of equilibrium (3), i.e.

$$\Delta\ddot{U} = -\eta\Delta\ddot{U}_g(t) - [C\Delta\dot{U}(t) + K(t)\Delta U(t) - b\Delta F(t)] \tag{10}$$

Thus, the responses of the structure can be evaluated step by step at successive increments of time, assuming that the properties of the system remain constant during the time step of analysis.

DOI: 10.1002/stc

For large structures, such as the highway bridge under consideration, the stiffness of some elements is likely to change during some of the calculation steps. Hence, the new configuration may not satisfy the equilibrium. As a result, the assumption of constant stiffness during a single time step may introduce significant errors. The one-step unbalanced force correction technique is not physically accurate and in some cases may produce significant numerical drift [26]. In order to correct this problem, an iterative procedure for automatically adjusting time stepping based on the half-step residual is used. In this method, the convergence tolerance should be specified carefully to achieve a sufficiently accurate solution within a reasonable computation time.

5. MATLAB IMPLEMENTATION OF NONLINEAR ANALYSIS

Although MATLAB offers a wide range of efficient tools for the integration of ordinary differential equations, it cannot deal with nonlinear system considered in this paper effectively. Therefore, a MATLAB-based nonlinear structural analysis tool has been developed for vibration control simulation of the seismically excited highway bridge. This nonlinear analysis tool is written as an S-function and is incorporated into the SIMULINK model of the benchmark bridge. The S-function solves the incremental equations of motion in Equation (3) using the previously discussed Newmark constant-average acceleration method and convergence technique at overshooting regions. The inputs to the S-function block in SIMULINK are the seismic excitation and the control forces provided by the control devices. The nonlinear analysis tool will remain invariant to the various control strategies developed and implemented. The efficiency of the procedure has been verified by several numerical examples and results of the ABAQUS model.

6. CONTROL DESIGN PROBLEM

The participants in the benchmark study are required to define the type, model and location of the control devices/sensor(s) and control algorithm(s) used in their proposed control strategies. The control device(s), sensor device(s) and control algorithms are interfaced to the structural evaluation model through measurement and device connection outputs, designated by y_m and y_c, respectively. The participants are required to specify the components of y_m and y_c in input files. The evaluation outputs y_e are used for the calculation of performance indices and are specified within the benchmark problem statement.

The evaluation model for the highway bridge representing the relationship between inputs, outputs and states is generally expressed in the following form:

$$\dot{x} = g_1(x, f, \ddot{u}_g, t) \tag{11}$$

$$y_e = g_2(x, f, \ddot{u}_g, t) \tag{12}$$

$$y_m = g_3(x, f, \ddot{u}_g, t) \tag{13}$$

$$y_c = g_4(x, f, \ddot{u}_g, t) \tag{14}$$

where x is the continuous-time state vector of the sensor(s) and y_e, y_m and y_c are vectors corresponding to the regulated responses, measured responses and output responses, respectively, which are used for control device model. Equation (11) is a highly a nonlinear equation and is expressed in state-space form.

DOI: 10.1002/stc

6.1. Sensor models

When active or semi-active control strategies are employed, the designer should describe and model the sensors to measure the outputs of the evaluation model in the following form:

$$\dot{x}^{\mathrm{s}} = g_5(x^{\mathrm{s}}, y_{\mathrm{m}}, f_{\mathrm{m}}, t) \tag{15}$$

$$y^{\mathrm{s}} = g_6(x^{\mathrm{s}}, y_{\mathrm{m}}, f_{\mathrm{m}}, v, t) \tag{16}$$

where x^{s} is the continuous-time state vector of the sensor(s), y^{s} is the continuous-time output of the sensor(s) in units of volts, y_{m} is a vector of measured outputs, f_{m} is the continuous-time output vector from the control device model, which may consist of device forces, or device stroke, and/or device acceleration needed for feedback into the controller, and v is the measurement noise vector.

6.2. Control algorithm

For active, semi-active or hybrid control systems, the corresponding discrete-time control algorithm may be expressed as

$$x^{\mathrm{c}}_{k+1} = g_7(x^{\mathrm{c}}_k, y^{\mathrm{s}}_k, k) \tag{17}$$

$$u_k = g_8(x^{\mathrm{c}}_k, y^{\mathrm{s}}_k, k) \tag{18}$$

where x^{c}_k is the discrete-time state vector of the control algorithm at each sampling time $t = kT$, y^{s}_k is the sampled input to the control algorithms, which is the discretized and quantized sensor model output, and u_k is the discrete control command from the control algorithm.

6.3. Control device(s)

Dynamic models of the control devices are not necessarily required in the design of control algorithms, although the participants are strongly encouraged to include device dynamics in the design of controllers. The device models can be interfaced with the bridge model as follows:

$$f = g_9(y_{\mathrm{c}}, u_k, t) \tag{19}$$

$$y_f = g_{10}(y_{\mathrm{c}}, u_k, t) \tag{20}$$

where f is the continuous-time force output of the control device(s) in units of N, y_f is the continuous-time response quantities from the evaluation model, which influence the control forces, and y_{c} is the continuous-time responses from the evaluation model, which are used as inputs to control device models.

If the dynamics of the control device(s) are considered, the device model can be presented as

$$\dot{x}^{\mathrm{d}} = g_{11}(x^{\mathrm{d}}, y_{\mathrm{c}}, u_k, t) \tag{21}$$

$$f = g_{12}(x^{\mathrm{d}}, y_{\mathrm{c}}, u_k, t) \tag{22}$$

$$y_f = g_{13}(x^{\mathrm{d}}, y_{\mathrm{c}}, u_k, t) \tag{23}$$

where x^{d} represents the continuous-time states of the control devices. Figure 8 provides the SIMULINK model used for evaluation of proposed control strategies. The participants in this benchmark study should follow the procedure summarized in Figure 9 to develop and evaluate their proposed control strategies.

DOI: 10.1002/stc

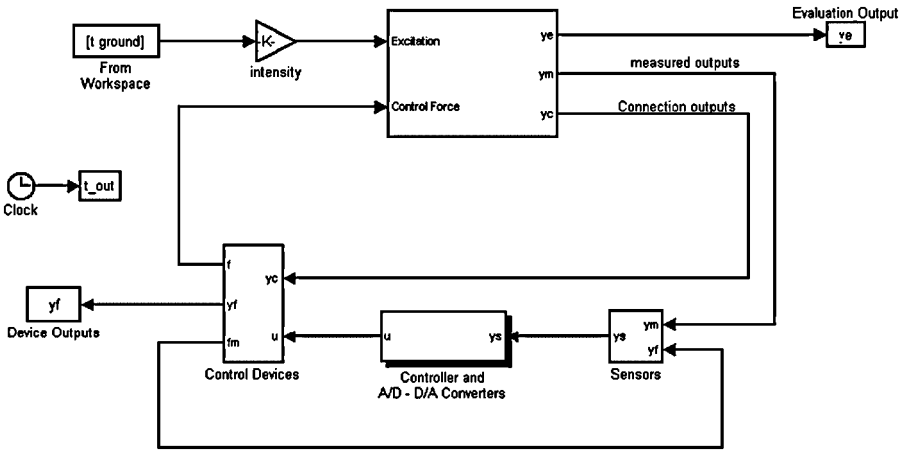

Figure 8. SIMULINK model for benchmark highway bridge problem.

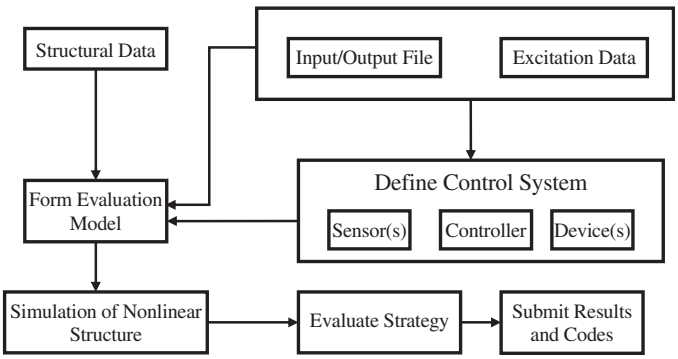

Figure 9. Flowchart of benchmark solution procedure.

7. EVALUATION CRITERIA

A set of 21 evaluation criteria to evaluate the effectiveness of different control devices and algorithm has been developed. These evaluation criteria are divided into three categories: peak responses, normed responses and control requirements.

The first eight evaluation criteria are defined to measure the reduction in peak response quantities of the benchmark bridge:

(i) Peak base shear force in the controlled structure normalized by the corresponding base shear in the uncontrolled structure:

$$J_1 = \max\left\{\frac{\max_{i,t}|F_{bi}(t)|}{F_{0b}^{\max}}\right\}, \quad i = 1,2 \text{ for } x \text{ and } y \text{ directions, respectively} \tag{24}$$

where $F_{bi}(t)$ is the base shear in the controlled structure for the ith case and $F_{0b}^{\max}$ is the maximum of the base shears in x and y directions in the uncontrolled structure for a prescribed earthquake.

DOI: 10.1002/stc

(ii) Peak overturning moment in the controlled structure normalized by the corresponding moment in the uncontrolled structure:

$$J_2 = \max\left\{\frac{\max_{i,t}\,|M_{bi}(t)|}{M_{0b}^{\max}}\right\}, \quad i = 1,2 \text{ for } x \text{ and } y \text{ directions, respectively} \tag{25}$$

where $M_{bi}(t)$ is the overturning moment in the controlled structure for the ith case and $M_{0b}^{\max}$ is the maximum of the overturning moments in x and y directions in the uncontrolled structure for a prescribed earthquake.

(iii) Peak displacement at the midspan of the controlled structure normalized by the corresponding midspan displacement of the uncontrolled structure:

$$J_3 = \max\left\{\max_{i,t}\left|\frac{y_{mi}(t)}{y_{0m}^{\max}}\right|\right\}, \quad i = 1,2 \text{ for } x \text{ and } y \text{ directions, respectively} \tag{26}$$

where $y_{mi}(t)$ is the displacement at the midspan of the controlled structure for the ith case and $y_{0m}^{\max}$ is the maximum of the midspan displacements in x and y directions in the uncontrolled structure for a prescribed earthquake.

(iv) Peak acceleration at the midspan of the controlled structure normalized by the corresponding peak midspan acceleration of the uncontrolled structure:

$$J_4 = \max\left\{\max_{i,t}\left|\frac{\ddot{y}_{mi}(t)}{\ddot{y}_{0m}^{\max}}\right|\right\}, \quad i = 1,2 \text{ for } x \text{ and } y \text{ directions, respectively} \tag{27}$$

where $\ddot{y}_{mi}(t)$ is the acceleration at the midspan of the controlled structure for the ith case and $\ddot{y}_{0m}^{\max}$ is the maximum of the midspan accelerations in x and y directions in the uncontrolled structure for a prescribed earthquake.

(v) Peak deformation of bearings in the controlled structure normalized by the corresponding peak deformation of bearings in the uncontrolled structure:

$$J_5 = \max\left\{\max_{i,t}\left|\frac{y_{bi}(t)}{y_{0b}^{\max}}\right|\right\}, \quad i = 1,2 \text{ for } x \text{ and } y \text{ directions, respectively} \tag{28}$$

where $y_{bi}(t)$ is the deformation of bearings in the controlled structure for the ith case and $y_{0b}^{\max}$ is the maximum of the bearing deformations in x and y directions in the uncontrolled structure for a prescribed earthquake.

(vi) Peak curvature at the bent column in the controlled structure normalized by the corresponding curvature in the uncontrolled structure:

$$J_6 = \max\left\{\max_{j,t}\frac{|\Phi_j(t)|}{\Phi^{\max}}\right\} \tag{29}$$

where $\Phi_j(t)$ is the curvature of the jth element in the nonlinear (bottom) region of piers and $\Phi_{\max}$ is the maximum curvature for a prescribed earthquake.

(vii) Peak dissipated energy of curvature at the bent column in the controlled structure normalized by the corresponding dissipated energy in the uncontrolled structure:

$$J_7 = \max\left\{\frac{\max_{j,t}\int \mathrm{d}E_j}{E^{\max}}\right\} \tag{30}$$

where $\mathrm{d}E_j$ is the dissipated energy of curvature at the jth element of the bent column in the controlled structure and $E^{\max}$ is the maximum energy dissipated in the uncontrolled structure for a prescribed earthquake.

DOI: 10.1002/stc

(viii) The number of plastic connections with control normalized by the corresponding number of plastic connections without control:

$$J_8 = \max\left\{\frac{N_{\mathrm{d}}^{\mathrm{c}}}{N_{\mathrm{d}}}\right\} \tag{31}$$

where $N_{\mathrm{d}}^{\mathrm{c}}$ and N_{d} are the number of plastic connections (hinges) in controlled and uncontrolled structures, respectively.

The second sets of six criteria are based on normed responses over the entire time duration of an earthquake. The normed value of the response, denoted by $\|\cdot\|$, is defined as

$$\|\cdot\| = \sqrt{\frac{1}{t_f}\int_0^{t_f} (\cdot)^2 \,\mathrm{d}t} \tag{32}$$

where t_f is the time required for the response to attenuate. Response quantities used to define the second set of evaluation criteria in the following equations are already defined in Equations (24)–(29):

(ix) Normed base shear force in the controlled structure normalized by the corresponding normed shear in the uncontrolled structure:

$$J_9 = \max\left\{\frac{\max_{i,t} \|F_{\mathrm{b}i}(t)\|}{\|F_{0\mathrm{b}}^{\max}\|}\right\} \tag{33}$$

(x) Normed overturning moment in the controlled structure normalized by the corresponding overturning in the uncontrolled structure:

$$J_{10} = \max\left\{\frac{\max_{t,i} \|M_{\mathrm{b}i}(t)\|}{\|M_{0\mathrm{b}}^{\max}\|}\right\} \tag{34}$$

(xi) Normed displacement at the midspan in the controlled structure normalized by the corresponding normed displacement at the midspan in the uncontrolled structure:

$$J_{11} = \max\left\{\max_i \frac{\|y_{\mathrm{m}i}(t)\|}{\|y_{0\mathrm{m}}^{\max}\|}\right\} \tag{35}$$

(xii) Normed acceleration at the midspan in the controlled structure normalized by the corresponding normed acceleration at the midspan in the uncontrolled structure:

$$J_{12} = \max\left\{\max_i \left\|\frac{\ddot{y}_{\mathrm{m}i}(t)}{\ddot{y}_{0\mathrm{m}}^{\max}}\right\|\right\} \tag{36}$$

(xiii) Normed deformation of bearings in the controlled structure normalized by the corresponding normed displacement of bearings in the uncontrolled structure:

$$J_{13} = \max\left\{\max_i \left\|\frac{y_{\mathrm{b}i}(t)}{y_{0\mathrm{b}}^{\max}}\right\|\right\} \tag{37}$$

(xiv) Normed curvature at the bent column in the controlled structure normalized by the corresponding normed curvature at the bent column in the uncontrolled structure:

$$J_{14} = \max\left\{\max_{j,t} \frac{\|\Phi_j(t)\|}{\|\Phi^{\max}\|}\right\} \tag{38}$$

DOI: 10.1002/stc

The last seven evaluation criteria are for quantifying a measure of control resource required by the controller itself:

(xv) Peak control force generated by the control device(s) normalized by the seismic weight of the bridge based on the mass of superstructure (excluding the foundation):

$$J_{15} = \max\left\{\max_{l,t}\left(\frac{f_l(t)}{W}\right)\right\} \tag{39}$$

where $f_l(t)$ is the force applied by the lth control device and W is the seismic weight of the bridge.

(xvi) Peak stroke of the control device(s) normalized by the maximum deformation of bearings in the uncontrolled structures:

$$J_{16} = \max\left\{\max_{l,t}\left(\frac{d_l(t)}{y_{0b}^{\max}}\right)\right\} \tag{40}$$

where $d_l(t)$ is the stroke of the lth control device.

(xvii) Peak instantaneous power required by the control device(s) normalized by the product of the weight and the maximum velocity of the bearing in the uncontrolled structure:

$$J_{17} = \max\left\{\frac{\max_t\left[\sum_l P_l(t)\right]}{\dot{y}_{0b}^{\max} W}\right\} \tag{41}$$

where P_l(t) is the power required by the lth control device and $\dot{y}_{0b}^{\max}$ is the maximum velocity of the bearing in the uncontrolled structure.

(xviii) Peak total power required for the control of the bridge normalized by the product of the weight and the maximum deformation of bearings in the uncontrolled structure:

$$J_{18} = \max\left\{\frac{\sum_l \int_0^{t_f} P_l(t)\,\mathrm{d}t}{y_{0b}^{\max} W}\right\} \tag{42}$$

(xix) Number of control devices:

$$J_{19} = \text{Number of control devices} \tag{43}$$

(xx) Number of sensors:

$$J_{20} = \text{Number of required sensors} \tag{44}$$

(xxi) Dimension of the discrete state vector required for the control algorithm:

$$J_{21} = \dim(x_k^c) \tag{45}$$

Notice that when passive control devices are used, the criteria J_{17} and J_{18} are zero and J_{20} and J_{21} are not considered. A summary of the evaluation criteria is presented in Table II. For each control design, these evaluation criteria should be calculated and evaluated for all the earthquakes provided in this benchmark problem. All criteria should be reported for each proposed control strategy. The participants are encouraged to specify their own additional criteria in their results to highlight the merits/advantages of the proposed control strategies. To demonstrate the effectiveness of a controller to different types of ground motion, evaluation criteria should be calculated using the same controller for all earthquake ground motions prescribed.

DOI: 10.1002/stc

Table II. Summary of the evaluation criteria.

Peak responses	Normed responses	Control strategy
Base shear	*Base shear*	*Peak force*
$J_1 = \max\left\{\frac{\max_{i,t}\lvert F_{bi}(t)\rvert}{F_{0b}^{\max}}\right\}$	$J_9 = \max\left\{\frac{\max_t \lVert F_{bi}(t)\rVert}{\lVert F_{0b}^{\max}\rVert}\right\}$	$J_{15} = \max\left\{\max_{l,t}\left(\frac{f_l(t)}{W}\right)\right\}$
Overturning moment	*Overturning moment*	*Device stroke*
$J_2 = \max\left\{\frac{\max_{i,t}\lvert M_{bi}(t)\rvert}{M_{0b}^{\max}}\right\}$	$J_{10} = \max\left\{\frac{\max_t \lVert M_{bi}(t)\rVert}{\lVert M_{0b}^{\max}\rVert}\right\}$	$J_{16} = \max\left\{\max_{l,t}\left(\frac{d_l(t)}{y_{0b}^{\max}}\right)\right\}$
Displacement at midspan	*Displacement at midspan*	*Peak power*
$J_3 = \max\left\{\max_{i,t}\left\lvert\frac{y_{mi}(t)}{y_{0m}^{\max}}\right\rvert\right\}$	$J_{11} = \max\left\{\max_i \frac{\lVert y_{mi}(t)\rVert}{\lVert y_{0m}^{\max}\rVert}\right\}$	$J_{17} = \max\left\{\frac{\max_t[\sum_l P_l(t)]}{y_{0b}^{\max} W}\right\}$
Acceleration at midspan	*Acceleration at midspan*	*Total power*
$J_4 = \max\left\{\max_{i,t}\left\lvert\frac{\ddot{y}_{mi}(t)}{\ddot{y}_{0m}^{\max}}\right\rvert\right\}$	$J_{12} = \max\left\{\max_i \left\lVert\frac{\ddot{y}_{mi}(t)}{\ddot{y}_{0m}^{\max}}\right\rVert\right\}$	$J_{18} = \max\left\{\frac{\sum_l \int_0^{t_f} P_l(t)\,\mathrm{d}t}{y_{0b}^{\max} W}\right\}$
Bearing deformation	*Displacement at abutment*	*Control devices*
$J_5 = \max\left\{\max_{i,t}\left\lvert\frac{y_{bi}(t)}{y_{0b}^{\max}}\right\rvert\right\}$	$J_{13} = \max\left\{\max_i \left\lVert\frac{y_{bi}(t)}{y_{0b}^{\max}}\right\rVert\right\}$	$J_{19} =$ Number of control devices
Ductility	*Ductility*	*Sensors*
$J_6 = \max\left\{\max_{j,t}\frac{\lvert\Phi_j(t)\rvert}{\Phi^{\max}}\right\}$	$J_{14} = \max\left\{\max_{j,t}\frac{\lVert\Phi_j(t)\rVert}{\lVert\Phi^{\max}\rVert}\right\}$	$J_{20} =$ Number of required sensors
Dissipated energy	*Plastic connections*	*Computational resource*
$J_7 = \max\left\{\frac{\max_{j,t}\int \mathrm{d}E_j}{E^{\max}}\right\}$	$J_8 = \max\left\{\frac{N_d^c}{N_d}\right\}$	$J_{21} = \dim(x_k^c)$

8. EARTHQUAKE EXCITATIONS

Six earthquake ground motions are selected for the highway bridge. These earthquakes are: North Palm Springs (1986), TCU084 component of Chi-Chi earthquake, Taiwan (1999), El Centro component of 1940 Imperial Valley earthquake, Rinaldi component of Northridge (1994) earthquake, Bolu component of Duzce, Turkey (1999), earthquake and Nishi-Akashi component of Kobe (1995) earthquakes. Table III lists important parameters of these ground motions. These earthquakes cover the soil type from A to D based on NEHRP classification. Time histories of these earthquakes are shown in Figure 10. All the earthquakes are used at the full intensity for the evaluation of the performance of the proposed control strategy. The uncontrolled responses of the benchmark highway bridge for all these earthquakes are provided in Table IV, which can be used to normalize the evaluation criteria.

9. CONTROL IMPLEMENTATION CONSTRAINTS AND PROCEDURES

To allow the participants of the benchmark study to compare and contrast various control strategies, the following implementation constraints and procedures are imposed on the proposed controller design proposed by the researchers:

(I) The outputs that are available for direct measurement in determining the control action are the absolute accelerations of the bridge at the nodes of the finite-element model, displacements of bearings and control device outputs, which are readily available (e.g. device stroke, force or absolute acceleration). In addition, absolute

DOI: 10.1002/stc

Table III. Properties of selected earthquake records.

Recording station	Earthquake	Magnitude	Distance to fault	Peak acceleration (g)	Peak velocity (cm/s)	Soil type
North Palm Springs	1986 North Palm Springs	6.0	7.3	0.492 (0.612)	73.3 (33.8)	A
TCU084	1999 Chi-Chi	7.6	10.39	1.157 (0.417)	114.7 (45.6)	B
El Centro	1940 Imperial Valley	7.0	8.3	0.313 (0.215)	29.8 (30.2)	C
Rinaldi	1994 Northridge	6.7	7.1	0.838 (0.472)	166.1 (73.0)	C
Bolu	1999 Duzce, Turkey	7.1	17.6	0.728 (0.822)	56.4 (62.1)	C
Nishi-Akashi	1995 Kobe	6.9	11.1	0.509 (0.503)	37.3 (36.6)	D

Peak acceleration and velocity values are for the EW component. The values of the NS components are shown in parentheses.

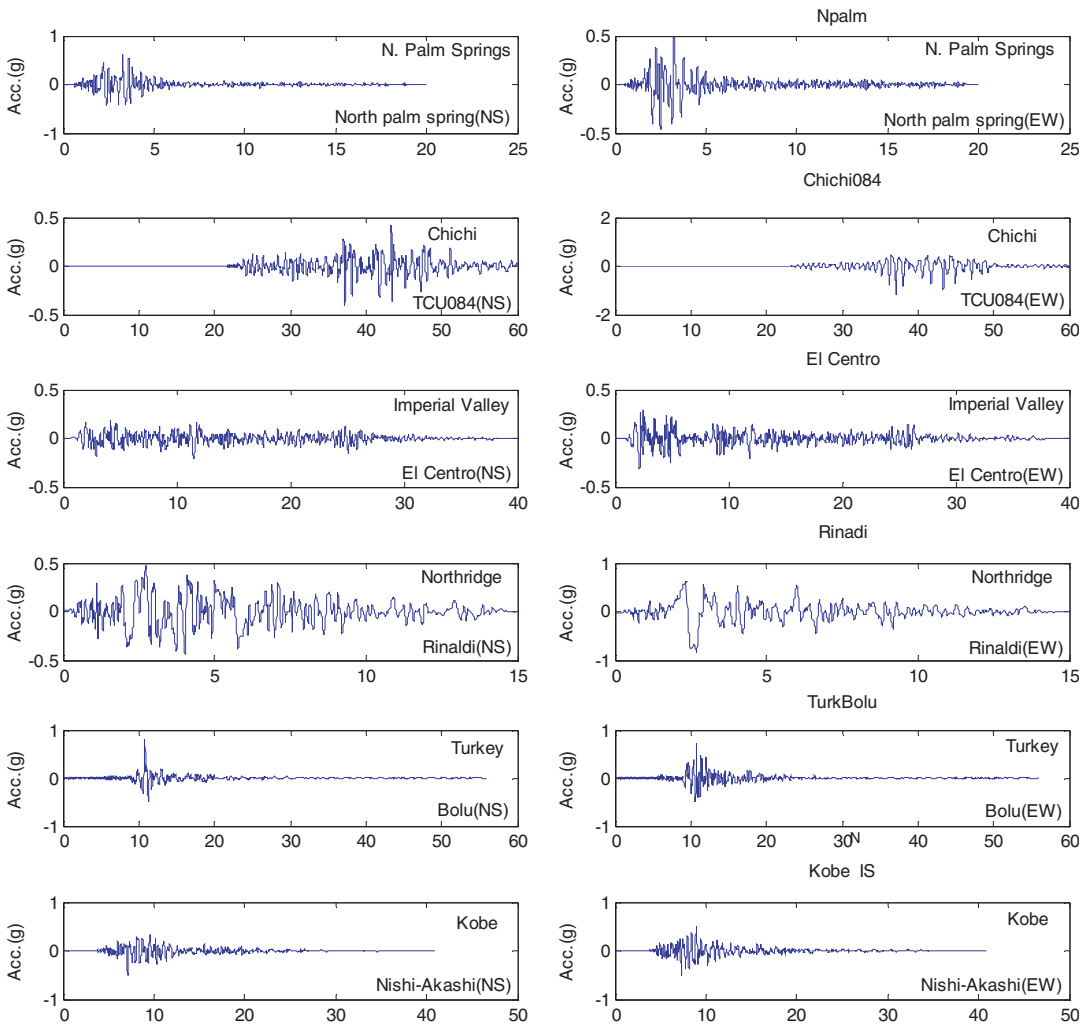

Figure 10. Two components of time histories of earthquake records.

DOI: 10.1002/stc

Table IV. Uncontrolled response quantities of the benchmark highway bridge.

Responses	North Palm Springs	Chi-Chi	El Centro	Northridge	Turkey	Kobe
F_{0b}^{max} (N)	5.8971×10^6	1.8691×10^7	5.8112×10^6	1.9403×10^7	1.2732×10^7	6.8987×10^6
M_{0b}^{max} (N m)	2.7647×10^7	5.5321×10^7	2.5832×10^7	5.6094×10^7	5.2548×10^7	3.3262×10^7
y_{0m}^{max} (m)	6.1958×10^{-2}	2.9221×10^{-1}	5.6767×10^{-2}	3.1035×10^{-1}	1.8147×10^{-1}	7.5226×10^{-2}
$\ddot{y}_{0m}^{max}$ (m/s^2)	5.7149	13.0790	3.7773	14.4120	9.8472	5.4297
y_{0b}^{max} (m)	9.3707×10^{-2}	2.9926×10^{-1}	1.0054×10^{-1}	3.1604×10^{-1}	1.9015×10^{-1}	1.5969×10^{-1}
Φ^{max}	1.3222×10^{-3}	2.4498×10^{-2}	1.2354×10^{-3}	2.9147×10^{-2}	1.1411×10^{-2}	1.5907×10^{-3}
E^{max}	0	2.1445×10^7	0	4.1298×10^6	1.1195×10^6	0
N_d	0	6	0	4	3	0
$\|\|F_{0b}^{max}\|\|$ (N)	1.0686×10^6	3.2961×10^6	1.3753×10^6	3.9129×10^6	1.4090×10^6	1.3165×10^6
$\|\|M_{0b}^{max}\|\|$ (N m)	5.2942×10^6	1.7637×10^7	6.6097×10^6	1.9231×10^7	1.2362×10^7	6.0719×10^6
$\|\|y_{0m}^{max}\|\|$ (m)	1.1767×10^{-2}	5.0797×10^{-2}	1.4804×10^{-2}	5.7892×10^{-2}	2.3291×10^{-2}	1.3733×10^{-2}
$\|\|\ddot{y}_{0m}^{max}\|\|$ (m/s^2)	1.0670	2.4918	0.9034	2.8937	0.9794	0.8692
$\|\|y_{0b}^{max}\|\|$ (m)	2.5421×10^{-2}	5.0754×10^{-2}	2.1701×10^{-2}	5.8469×10^{-2}	3.3114×10^{-2}	3.4177×10^{-2}
$\|\|\Phi^{max}\|\|$	2.5319×10^{-4}	5.2955×10^{-3}	3.1610×10^{-4}	4.8558×10^{-3}	6.1383×10^{-3}	2.9038×10^{-4}
x^{max} (m)	9.7351×10^{-2}	3.1254×10^{-1}	1.0933×10^{-1}	3.4697×10^{-1}	1.9181×10^{-1}	1.6197×10^{-1}
$\dot{x}^{max}$ (m/s)	1.1310	2.1522	8.2198×10^{-1}	2.3611	1.9672	1.4553

velocity measurements may be added by filtering the measured accelerations as described in [2]. If pseudo-velocity measurements are used, the participants should specify the filter used in the sensor model.

(II) The controller proposed for the benchmark highway bridge is digitally implemented with a sampling time between 0.001 and 0.005 s, which should be set equal to the integration step of the simulation.

(III) The A/D and D/A converters on the digital controller have 16-bit precision and a span of ± 10 V.

(IV) Each of the measured responses contains a root mean-square noise of 0.03 V, which is approximately 0.3% of the full span of the A/D converters. The measurement noises are modeled as Gaussian rectangular pulse processes with a pulse width equal to the integration step.

(V) Although the sensors can be installed at any nodes of the FEM of the bridge, all control devices should be placed between the deck and the end abutments of the bridge. There is no limitation on the number of sensors and devices that can be utilized in the benchmark study.

(VI) The designer of the controller must justify that the proposed algorithm can be implemented with currently available hardware and computational resources.

(VII) The control algorithm is required to be stable and closed-loop stability should be ensured.

DOI: 10.1002/stc

(VIII) When control device dynamics are included, the control signal to each device should be less than or equal to the maximum span of D/A converters.

(IX) The capabilities of each control device employed should be considered. The participants must demonstrate that this force constraint is met during each of the earthquakes.

(X) The control algorithm must be implemented for all earthquake records and results presented in terms of the performance criteria specified in the benchmark problem.

(XI) The participants of this study are requested to submit electronically a complete set of MATLAB files used for their control strategies.

(XII) Any additional constraints that are unique to each control scheme should also be reported. Detailed work on the derivation of reduced order models for controller design and the design of sample passive, semi-active and active controllers is presented in Tan and Agrawal [27]. In this Phase I benchmark problem, bridge superstructure (deck) is fixed to the outrigger in the center of the bridge. The Phase II benchmark problem in which the bridge superstructure is isolated from the outrigger is presented in Nagarajaiah [28].

10. CONCLUSIONS

A benchmark problem on structural response control of highway bridge has been developed. The model is based on the 91/5 highway over-crossing in southern California. A 3D finite-element model of the highway over-crossing has been developed. The nonlinear evaluation model has been developed to model the material nonlinearity of center bent columns and isolation bearings. A new nonlinear dynamic analysis program has been developed and made available to facilitate direct comparison of results of various control algorithms. A set of evaluation criteria is defined and control constraints are presented in this paper. The benchmark problem package can be downloaded from the URL http://www-ce.engr.ccny.cuny.edu/People/Agrawal/index.htm. More information on this problem can be obtained by contacting the first author (Dr Agrawal) at Tel.: +1 212 650 8442. E-mail: Agrawal@ccny.cuny.edu

ACKNOWLEDGEMENTS

The research presented in this paper is supported by the National Science Foundation Grant Number CMS 0099895. Any opinions, findings and conclusions or recommendations expressed in this material are those of the authors and do not necessarily reflect those of National Science Foundation. The authors sincerely acknowledge the feedback by the members of the ASCE Committee on Structural Control and the International Association of Structural Control and Monitoring.

REFERENCES

1. Caughey TK. The benchmark problem. *Earthquake Engineering & Structural Dynamics* 1998; **27**(11):1125.
2. Spencer Jr BF, Dyke SJ, Deoskar HS. Benchmark problems in structural control—part I: active mass driver system, and part II: active tendon system. *Earthquake Engineering & Structural Dynamics* 1998; **27**(11):1127–1139, 1141–1147.

DOI: 10.1002/stc

3. Spencer Jr BF, Christenson RE, Dyke SJ. Next generation benchmark control problem for seismically excited buildings. *Proceedings of the Second World Conference on Structural Control*, Kyoto, Japan, 29 June–2 July 1999; 1351–1360.
4. Ohtori Y, Christenson RE, Spencer Jr BF, Dyke SJ. Benchmark control problems for seismically excited nonlinear buildings. *Journal of Engineering Mechanics* 2004; **130**(4):366–385.
5. Yang JN, Agrawal A, Samali B, Wu JC. Benchmark problem for response control of wind excited tall buildings. *Journal of Engineering Mechanics* 2004; **130**(4):437–446.
6. Dyke SJ, Caicedo JM, Turan G, Bergman LA, Hague S. Phase I benchmark control system for seismic response of cable-stayed bridges. *Journal of Structural Engineering* 2003; **129**(7):857–872.
7. Caicedo JM, Dyke SJ, Moon SJ, Bergman LA, Turan G, Hague S. Phase II benchmark control problem for seismic response of cable-stayed bridges. *Journal of Structural Control* (*currently Journal of Structural Control and Health Monitoring*) 2003; **10**(3–4):137–168.
8. Narasimhan S, Nagarajaiah S, Gavin H, Johnson EA. Smart base-isolated benchmark building. Part I: problem definition. *Structural Control and Health Monitoring* 2006; **13**(2–3):573–588.
9. Nagarajaiah S, Narasimhan S. Smart base-isolated benchmark building. Part II: phase I sample controllers for linear isolation systems. *Structural Control and Health Monitoring* 2006; **13**(2–3):589–604.
10. Narasimhan S, Nagarajaiah S, Johnson EA. Structural control benchmark problem: phase II—nonlinear smart base-isolated building subjected to near-fault earthquakes. *Structural Control and Health Monitoring* 2008; **15**(5):653–656.
11. Narasimhan S, Nagarajaiah S, Johnson EA. Smart base-isolated benchmark building part IV: phase II sample controllers for nonlinear isolation systems. *Structural Control and Health Monitoring* 2008; **15**(5):657–672.
12. Yang JN, Kawashima K, Wu JC. Hybrid control of seismic-excited building structures. *Earthquake Engineering & Structural Dynamics* 1995; **24**:1437–1451.
13. Saharabudhe S, Nagarajaiah S. Semi-active control of sliding isolated bridges using MR dampers: an experimental and numerical study. *Earthquake Engineering & Structural Dynamics* 2005; **34**(8):965–983.
14. Tan P, Agrawal AK, Pan Y. Near-field effects on seismically excited highway bridge with nonlinear viscous dampers. *Journal of Bridge Structures* 2005; **1**(3):307–318.
15. Saiidi M, Maragakis E, Griffin G. Effect of base isolation on seismic response of multi-column bridges. *Structural Engineering and Mechanics* 1999; **8**:411–419.
16. Tsopelas P, Constantinou MC. Study on elastoplastic bridge seismic isolation system. *Journal of Structural Engineering* (ASCE) 1997; **123**(4):489–498.
17. Turkington DH, Carr AJ, Cooke N, Moss PJ. Seismic design of bridges on lead–rubber bearings. *Journal of Structural Engineering* (ASCE) 1988; **115**:3000–3016.
18. Feng MQ, Kim JM, Shinozuka M, Purasinghe R. Viscoelastic dampers at expansion joints for seismic protection of bridges. *Journal of Bridge Engineering* 2000; **5**(1):67–74.
19. Kawashima K, Unjoh S. Seismic response control of bridges by variable dampers. *Journal of Structural Engineering* 1994; **120**(9):2583–2601.
20. *ABAQUS*. Hibbit, Karlsson & Sorensen, Inc.: Pawucket, RI, 2003.
21. Makris N, Zhang J. Structural characterization and seismic response analysis of a highway overcrossing equipped with elastomeric bearings and fluid dampers: a case study. *Report No. PEER-2002-17*, Pacific Earthquake Engineering Research Center, University of California, Berkeley, CA, 2002.
22. *MATLAB*. The Math Works, Inc.: Natick, MA, 2002.
23. Cheng FY. Matrix analysis of structural dynamics. *Application and Earthquake Engineering*. Marcel Dekker: New York, 2001.
24. Newmark NM. A method of computation for structural dynamics. *Journal of the Engineering Mechanics Division* (ASCE) 1959; **85**(3):67–94.
25. Hilber HM, Hughes TJR, Taylor RL. Collocation, dissipation and 'overshoot' for time integration schemes in structural dynamics. *Earthquake Engineering & Structural Dynamics* 1978; **6**:99–117.
26. Villaverde R, Lamb RC. Scheme to improve numerical analysis of hysteretic dynamic systems. *Journal of Structural Engineering* (ASCE) 1989; **115**(1):228–233.
27. Tan P, Agrawal AK. Benchmark structural control problem for a seismically excited highway bridge—Part II: Phase I sample control design. *Structural Control and Health Monitoring* DOI: 10.1002/stc.300.
28. Nagarajaiah S, Narasimhan S, Agrawal AK, Ping T. Benchmark structural control problem for a seismically excited highway bridge—Part III: Phase II sample controller for the fully base-isolated case. *Structural Control and Health Monitoring* DOI: 10.1002/stc.293.